Fluorophore Concentration Controls the Homo-FRET Efficiency and Directionality across Proteins both in Solution and in Solid Protein Matrices

Yuval Agam, Ambili Ramanthrikkovil Variyam, and Nadav Amdursky*

Schulich Faculty of Chemistry, Technion – Israel Institute of Technology, Haifa 3200003, Israel.

*Corresponding author

Prof. Nadav Amdursky,

Schulich Faculty of Chemistry, Technion – Israel Institute of Technology, Haifa, 3200003, Israel

Tel: +972-4-8295953

e-mail: amdursky@technion.ac.il

Keywords

FRET, Fluorescein, Bovine serum albumin, Molecular doping

Abstract

Light harvesting in nature is one of the most important processes, starting with the absorption of light by chromophores within proteins and the transfer of energy from one another via the Förster resonance energy transfer (FRET) mechanism. If the energy is transferred between identical chromophores, the resulting is Homo-FRET. Here, we introduce an artificial system that allows us to control the number of chromophores within a certain protein and to decipher the mechanism of Homo-FRET in proteins in ways not possible in biological systems. We follow Homo-FRET by ultrafast fluorescence anisotropy measurements. We show that for solvated proteins, the mechanism, rate, and efficiency of Homo-FRET are highly dependent on the number of chromophores within the protein. However, in the solid protein matrix, the mechanism remains the same as the number of chromophores increases, but the solid matrix allows long-range Homo-FRET, resulting in full depolarization. The observed higher-than-ideal Homo-FRET contribution to the observed fluorescence anisotropy decay together with the reduction in the limiting anisotropy suggest a mixed coherent-incoherent mechanism of energy transfer.

Förster resonance energy transfer (FRET) occurs when excited-state energy from a donor fluorophore is transferred nonradiatively to an adjacent acceptor fluorophore in its ground state. FRET has two distinct categories. The first involves the participation of two fluorophores with differing emission spectra as the donor and acceptor, known as Hetero-FRET. The second classification of FRET, referred to as Homo-FRET, pertains to scenarios where both the donor and acceptor consist of the same type of fluorophore with identical spectra.[1, 2]

Homo-FRET has a substantial role in various biological systems, with the most notable example being the photosynthesis apparatus. When fluorophores such as chlorophyll are densely and effectively aligned within a protein structure, they can transfer energy with nearly perfect efficiency.[3-6] Due to the importance of this process for life on Earth, multiple theories have been proposed to explain the mechanism behind this remarkably efficient excitonic energy transfer.[4, 7-12] One of the limiting factors in exploring Homo-FRET across fluorophores within proteins is our inability to manipulate the chemical nature of the fluorophore in a facile manner or induce any alterations in the density of fluorophores in natural protein systems. In this work, we explore how energy is transferred between identical fluorophores in artificial protein systems, which gives us much freedom in controlling the number of fluorophores in the system and the environment of the system.

Here, we used the bovine serum albumin (BSA) protein as the host protein for the incorporation of fluorophores both into solvated proteins and within a solid-state protein matrix that was prepared using BSA. To construct a BSA-based solid matrix, we used the known ability of BSA to undergo electrospinning[13] and to make a solid mat capable of large water uptake.[14, 15] Another important property of BSA in our study is its ability to tightly bind a variety of molecules at many binding sites, and as discussed below, in this study, we bound fluorophores to BSA. Importantly, it was also shown that the BSA protein within the solid electrospun matrix can also retain the ability to strongly bind small molecules even though the protein is partially unfolded within the solid matrix.

For Homo-FRET to occur, the separation between donor and acceptor fluorophores typically needs to be within the range of less than 10 nm. Furthermore, the fluorophore should exhibit a small Stokes shift, ensuring that its absorption spectrum overlaps with its emission spectrum.[1] Several dyes are known for their ability to promote Homo-FRET under suitable conditions. A recent discovery indicated that the aggregation of fluorescein (Flu) in a solution can also sustain this form of energy transfer.[16] In this study, we chose Flu as the fluorophore within the BSA protein for mediating the expression of Homo-FRET. We chose Flu mainly because of its absorption and emission spectral overlap, although it also has other significant advantages, such as its high water solubility and high binding efficiency to the BSA protein.[17]

One of the most convenient experimental approaches for exploring Hetero-FRET systems is to measure the quenching of the donor's fluorescence lifetime in the presence of an acceptor. However, for Homo-FRET, this approach is far more challenging, as the involvement of identical fluorophores implies that there will be no change in the fluorescence lifetime even when energy transfer occurs. Accordingly, to explore Homo-FRET, one can use time-resolved anisotropy measurements.[1, 2, 18, 19] In this experimental method, polarized light is utilized for excitation, and the resulting fluorescence is measured in both parallel and perpendicular orientations relative to the electric field of the incident light.[20, 21] The optimal conditions for excitation occur when a fluorophore transition dipole is aligned parallel to the exciting light electric field[22]. Following excitation, the orientation of the fluorophore's transition dipole may evolve over time, consequently impacting the emitted fluorescence and creating depolarization. The predominant mechanism driving temporal orientation changes is molecular rotational motion. FRET-type energy transfer between an excited fluorophore and a neighboring fluorophore with a different transition dipole orientation can also cause significant orientation shifts.[2, 23] Accordingly, fluorescence anisotropy measurements can detect these orientation shifts and, thus, can be used as a tool to measure Homo-FRET.[20]

To test the feasibility of Homo-FRET between Flu molecules, we first measured the absorption and emission spectra of the molecule. Figure 1 shows the spectral overlap between the absorption and emission spectra of Flu, suggesting that the Homo-FRET process may occur between nearby molecules. Energy transfer occurs with a probability of 50% when the distance referred to as the average Förster radius (R_0) is reached. We calculated the average Förster radius for Flu to be 5.03 nm using Equation 1[24]:

$$R_0^6 = \left(\frac{9000(ln10)\kappa^2 Q_D}{128\pi^5 N n^4}\right) J \quad (1)$$

where Q_D is the Flu quantum yield ($Q_D = 0.92$)[25] and κ^2 is taken as $2/3$ assuming that the orientation of the fluorophore is random.[24] N is Avogadro constant and n is the refractive index of water (n =1.333). The overlap integral (J) represents the overlap of the Flu emission (F_D) and absorption spectra (ε_A) calculated using the measured spectra, giving J:

$$J = \int_0^\infty F_D(\lambda)\varepsilon_A(\lambda)\lambda^4 d\lambda = 9.74 \cdot 10^{14}\, M^{-1} cm^{-1} nm^4 \quad (2)$$

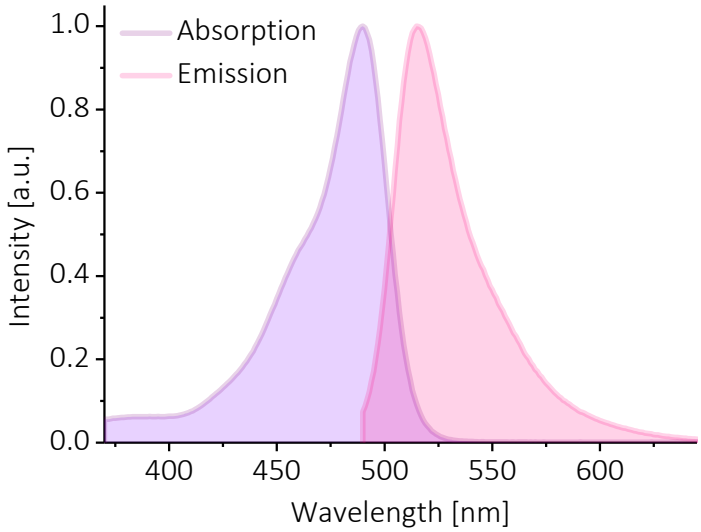

Figure 1. Absorption and emission spectra (λ_{ex}=480 nm) of Flu in water.

Once we established the possibility of Homo-FRET between Flu molecules, we followed this process using fluorescence anisotropy measurements. When subjected to vertically polarized light excitation, the anisotropy value is calculated using the following expression:

$$r = \frac{I_{\parallel} - G \cdot I_{\perp}}{I_{\parallel} + 2G \cdot I_{\perp}} \quad (3)$$

$I_{\parallel}$ and $I_{\perp}$ denote the intensities of polarized and depolarized emission, respectively, with factor G serving to rectify variations in the instrument detection efficiency for different emission polarizations.

Before diving into the experiment, we should first explain what we expect to observe. For a freely rotating fluorophore in a non-viscous solution, the emission dipole of the molecule upon excitation also freely rotates, thus resulting in rapid depolarization of the molecule (Figure 2a, top panel). This fast depolarization should result in a fast fluorescence anisotropy decay. However, if fluorophore motion is inhibited, e.g., by binding to a protein, we expect to observe a slow anisotropy decay resulting from the restricted motion of the fluorophore within the protein and the slow movement of the protein (Figure 2a, bottom panel).

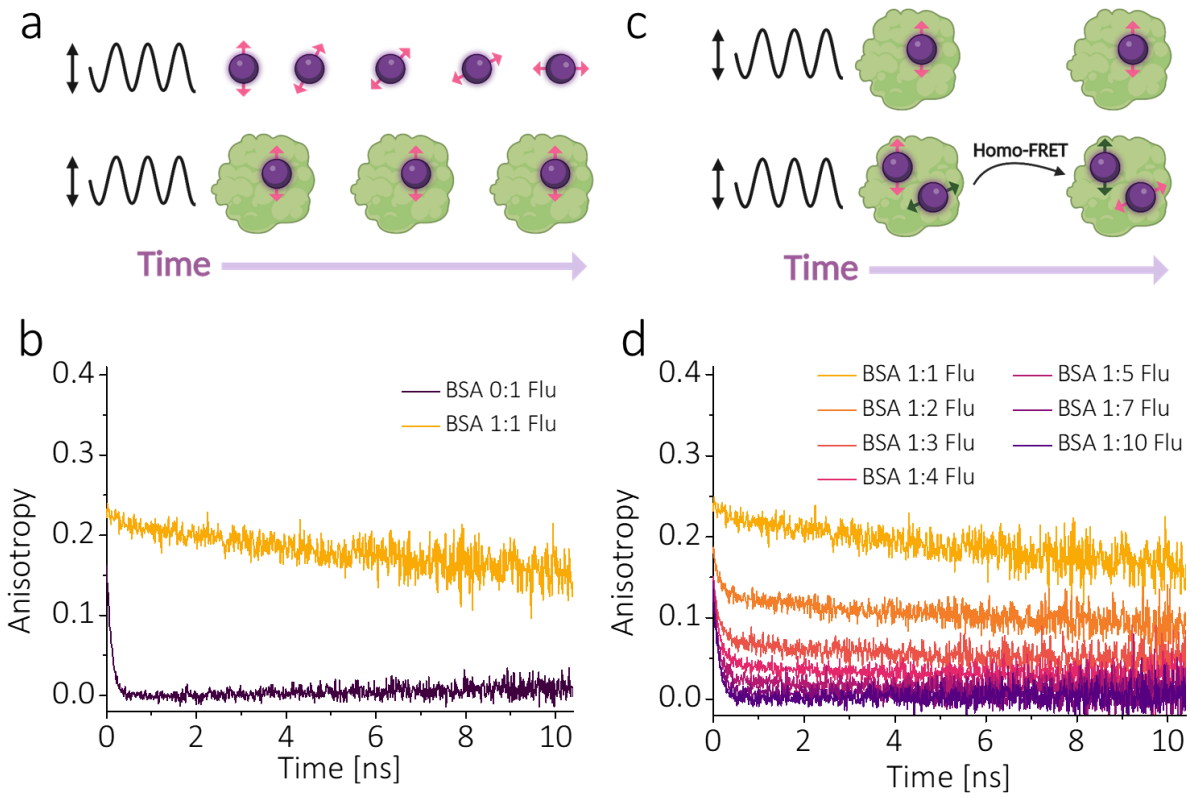

Figure 2. (a) Schematic of the rotation of fluorescence emission dipoles (pink arrows) over time, causing rapid depolarization after light excitation (top). Limited mobility within a large protein limits the fluorophores, significantly reducing depolarization over time (bottom). (b) Time-resolved anisotropy decays of Flu in water and in the Flu-BSA complex. (c) Schematic of the fluorescence emission dipoles (pink arrows) without Homo-FRET (top) or with (bottom) after introducing a neighboring fluorophore, causing fast depolarization after light excitation. (d) Time-resolved anisotropy decays of different numbers of Flu molecules inside each BSA protein. The excitation and emission wavelengths in (b) and (d) are 490 and 520 nm, respectively.

In our experiments, we first examined the anisotropy of free Flu molecules in an aqueous solution (Figure 2b, purple curve). The figure shows how the anisotropy rapidly decays as the Flu molecules freely rotate in water, i.e., a nonviscous solvent, as described above. As stated, we used BSA as the chosen protein for the binding of the Flu molecule. Indeed, following the binding of a single Flu molecule to each BSA protein (on average), which has the same Flu concentration as that used without BSA, we observed a very slow anisotropy decay (Figure 2b, yellow curve), which

corresponds to the restriction of the molecule's movement within the protein.[21] The major change in the measured anisotropy is also proof of the successful binding of the fluorophore to BSA.

For a Homo-FRET process to occur, the molecules must be packed at a distance that allows interaction. For our measurements of solvated Flu molecules in water, the low density of the molecules prevents energy transfer. For this reason, decreasing the distance between molecules is essential for obtaining Homo-FRET. In this study, we used the BSA protein as a platform for binding multiple Flu molecules, thus fixing their position at a distance of less than 10 nanometers from each other. As mentioned, we used fluorescence anisotropy measurements to examine whether or not Homo-FRET happened. If Homo-FRET occurs between two neighboring fluorophores, the energy transfer from one fluorophore to the other results in a rapid change in the emission dipole orientation, which is much faster than the restricted movement of the fluorophores themselves (Figure 2c).

In our experiments, the presence of several binding sites within BSA enabled us to increase the quantity of Flu molecules attached to each BSA molecule. At this stage, it was of utmost importance to verify that all the Flu molecules bound to the BSA protein and did not remain solvated in solution. Accordingly, we used filtering membranes to remove any excess unbound Flu molecules that could have been left in our system. Interestingly, we found that up to 10 Flu molecules can bind (on average) to a single BSA protein. The next step was to follow the change in the fluorescence anisotropy decay at different ratios of BSA to Flu molecules (Figure 2d). Already from the ratio of BSA:Flu of 1:2, we observed a faster decay component of the anisotropy compared to the BSA:Flu ratio of 1:1. Importantly, we noticed that adding more Flu molecules to one BSA protein resulted in a faster decay component of its anisotropy (Figure 2d), thus indicating an increase in the Homo-probability and rate of Homo-FRET. As an important control experiment, we also used another fluorophore, chlorophyll, which cannot bind to BSA molecules in quantities similar to those of the Flu molecule. This fluorophore showed a completely different trend in the anisotropy measurements as a function of the chlorophyll molecules in solution. In these control experiments, we observed a

'dip-and-rise' behavior in the anisotropy measurements, thus indicating that some of the fluorophores were bound to the BSA protein and that some were not[22, 24, 26, 27] bound to the BSA protein (Figure S1 and text within).

To describe the anisotropy decay for a spherical complex (i.e., a protein) having two or more close fluorophores, we used the following equation:

$$r(t) = r_0\left(a_{FRET}\cdot e^{-\frac{t}{\tau_1}} + a_{rot}\cdot e^{-\frac{t}{\tau_2}}\right) \quad (4)$$

where r_0 is the limiting anisotropy, τ_1 is the Homo-FRET correlation time, a_{FRET} is the fractional amplitude of the Homo-FRET decay component, τ_2 is the rotation correlation time, and a_{rot} is the fractional amplitude of the rotational decay component.

As shown in our results (Figure 2d), when Homo-FRET occurs, we observe initial rapid decay, which corresponds to the energy transfer process, followed by a slow component, which corresponds to the restricted motion of the fluorophore in our system. Accordingly, we fitted the decay curves with a double exponential fitting (Table 1, τ_1 and τ_2 values). For the protein sample containing a single Flu molecule, the data were fitted using a single exponent since no rapid component associated with Homo-FRET was observed. When two Flu molecules are within the protein, we can determine the efficiency of Homo-FRET using the following equation:

$$E = \frac{\kappa_T}{\tau^{-1} + \kappa_T} \quad (5)$$

where κ_T is the FRET transfer rate, which equals $\kappa_T = \frac{1}{2\tau_1}$ for a pair of fluorophores, assuming an identical transfer rate in both directions, τ_1 is the mentioned Homo-FRET correlation time, and τ = 3.97 ns (Figure S2) is the radiative fluorescence lifetime decay of a single Flu bound to BSA in an aqueous environment. Using Eq. (5), we calculated an efficiency of $E = 0.9$ for Homo-FRET between a pair of Flu molecules within solvated BSA proteins. Using the efficiency value, we can

also calculate the separation distance between the Flu molecules as r = 3.4 nm by using the following equation:

$$r^6 = R_0^6\left(\frac{1}{E} - 1\right) \quad (6)$$

When more than 2 Flu molecules were within the BSA protein, we observed a gradual increase in the Homo-FRET decay rate and an increase in the magnitude of the Homo-FRET (a_{FRET}). The sample containing 10 Flu molecules within each BSA did not conform to a double exponential fit due to complete depolarization resulting from Homo-FRET.

What does it mean a complete depolarization? To answer this question, we introduce the term 'cluster size' for the fluorophores within the protein. Adding more molecules to the cluster enhances the depolarization by inducing randomness in the orientation vector of the dipoles. Once energy exchange through Homo-FRET has reached a state of equilibrium within the cluster, the likelihood of photon emission becomes uniform across all fluorophores within the group. Thus, complete depolarization means that at the end of the Homo-FRET process, there is no preferred direction for the emission dipole within the cluster. When dealing with a cluster of size N, the anisotropy value following the Homo-FRET process is expected to decrease by $\frac{N-1}{N}$ of the initial r_0 value.[28] Hence, estimating the cluster size can be achieved by measuring the time-resolved anisotropy.[29] However, this estimation holds under specific circumstances: 1) The fluorophores are randomly oriented. 2) The depolarization resulting from rotation is considered to be negligible. 3) The energy transfer rate exceeds the fluorescence time. In our experiment, the fluorophores exhibit random orientations. The interaction with the large protein significantly extends the rotational time, and the lifetime of the Flu bound to the protein is 3.97 ns; hence, the energy transfer rate is much faster. Since our system conforms to all the criteria, we can examine how Homo-FRET contributes to the decay of anisotropy across various cluster sizes. This Homo-FRET contribution can be calculated by the percentage reduction in the anisotropy value following the fast Homo-FRET component compared to the initial

sample (BSA 1:1 Flu), which does not contain Homo-FRET (essentially, r_0). Ideally, this value (Δ_{FRET}) should theoretically decrease to 50%, 67%, 75%, 80%, 85%, and 90% when 2, 3, 4, 5, 7, and 10 Flu molecules are within BSA (Table 1). However, as shown in Table 1, our obtained values are in line with the theoretical values only when less than 4 Flu molecules were inside the BSA, and when more Flu molecules were inside the protein, the contribution of Homo-FRET was greater than expected. Our observation of a greater contribution of Homo-FRET than ideal for a large number of Flu molecules within the protein is highly interesting and unexpected in light of a previous work that showed a lower than theoretical contribution of Homo-FRET.[30] We claim here that the delocalization of energy across several fluorophores within BSA can explain this higher-than-ideal contribution from Homo-FRET. A further indication that might support the delocalization claim is the reduction in the r_0 values upon the addition of more Flu molecules to the protein. In the absence of any other incoherent Homo-FRET, i.e., the excitation energy hopping process that we observe, this limiting anisotropy should not change. However, if a very fast depolarization process occurs on a timescale below the resolution of the anisotropy experiments, it should result in a decrease in r_0.[30] This fast process can be ascribed to an energy transfer mechanism among closely situated and aligned fluorophores, leading to energy delocalization.[31] Above a certain ratio of BSA:Flu (>1:3), we 'saturate' the contribution of coherent processes, as can be observed by the constant r_0 from this point, which also indicates the point that we have started to observe the deviation of the contribution of Homo-FRET from the ideal values.

Table 1. Fitted rotation and Homo-FRET correlation time within solvated BSA proteins as a function of the number of Flu within the protein.

	$\tau_1(ns)$	$\tau_2(ns)$	r_0	a_{FRET}	Δ_{FRET}	$\Delta_{FRET}^{Theor.}$
BSA 1:1 Flu	---	28.2 ± 0.94	0.23	---	---	---
BSA 1:2 Flu	0.19 ± 0.03	28.9 ± 1.64	0.17	0.3	48	50
BSA 1:3 Flu	0.17 ± 0.02	22.03 ± 1.79	0.14	0.5	70	67
BSA 1:4 Flu	0.149 ± 0.008	20.28 ± 2.02	0.14	0.73	83	75
BSA 1:5 Flu	0.136 ± 0.008	19.32 ± 4.15	0.14	0.85	92	80
BSA 1:7 Flu	0.133 ± 0.007	17.7 ± 9	0.13	0.94	96	85
BSA 1:10 Flu	0.119 ± 0.005	---	0.13	1	~100	90

In the second part of our work, we switched from solvated proteins to solid-state protein matrices. While Homo-FRET between a cluster of fluorophores situated within a solvated protein is restricted by the size of the protein, Homo-FRET between fluorophores situated within macroscopic protein matrices does not have this restriction, thus enabling long-range distances within the matrix to be reached. To do so, we used the BSA protein to form a free-standing matrix by electrospinning[13] (Figure 3a). As stated, since the matrix platform is composed solely of proteins, it enables us to explore Homo-FRET within proteins across many proteins and not be confined to a single protein. Like the solvated BSA protein, the BSA matrix can also easily bind various small molecules from the solution in a molecular doping process by simply placing the matrix in the solution of the dopant[32, 33] (Figure 3b). By varying either the concentration of the dopant (fluorophore) in the doping solution or the duration of the doping process, we can easily control the final doping efficiency within the BSA matrix, i.e., the average distance between the fluorophores within the matrix. In line with the first part, we doped the BSA mat with Flu molecules at various concentrations of fluorophores, resulting in mats possessing distinct doping densities. We used UV–vis absorption spectra analysis to determine the resulting doping density in each sample (Table 2).

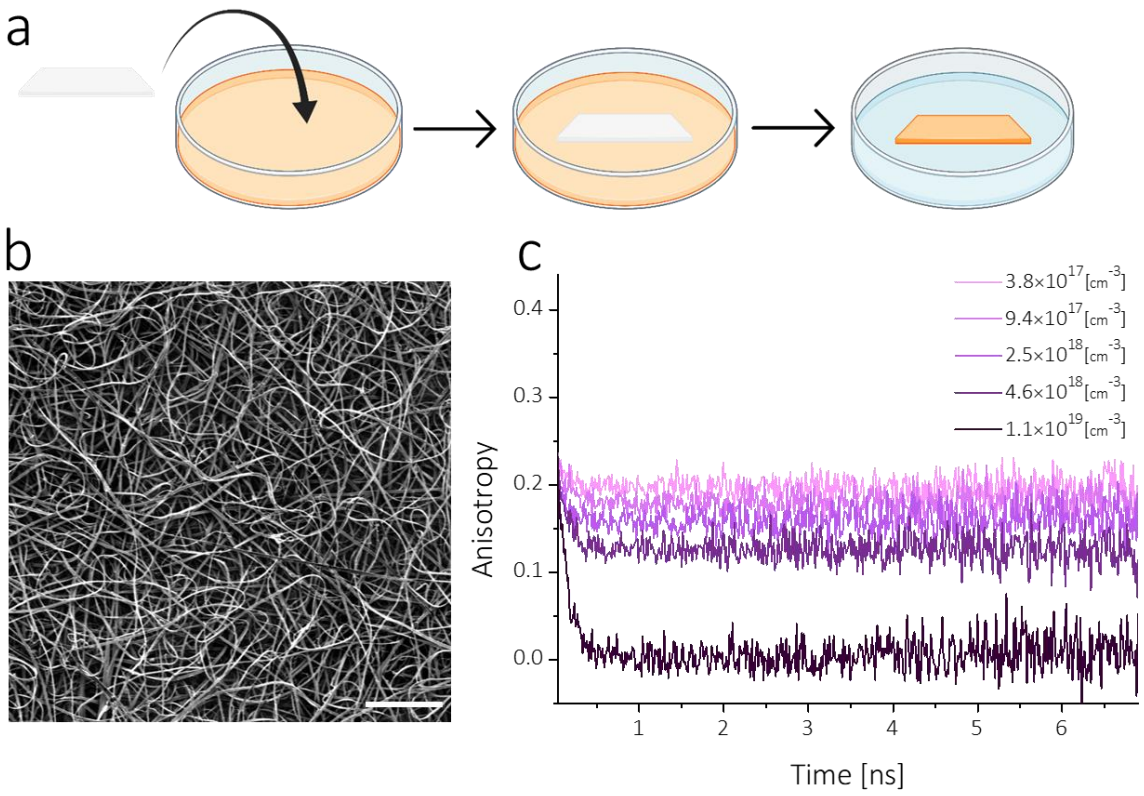

Figure 3. (a) Schematic of the doping process. (b) SEM image of the BSA mat; the scale represents 50 μm. (c) Time-resolved anisotropy decays for different Flu doping densities inside the BSA mat. The excitation and emission wavelengths are 490 and 520 nm, respectively.

Table 2. Fitted rotation and Homo-FRET correlation time for solid BSA mats with different doping densities of Flu.

Doping density $[cm^{-3}]$	r_∞	A_{FRET}	τ_3
$\mathbf{1.1 \times 10^{19}}$	0.19688	0.03997	0.12737 ± 0.035
$\mathbf{4.6 \times 10^{18}}$	0.17832	0.06804	0.12473 ± 0.028
$\mathbf{2.5 \times 10^{18}}$	0.1573	0.06706	0.11797 ± 0.024
$\mathbf{9.4 \times 10^{17}}$	0.12636	0.12291	0.12132 ± 0.012
$\mathbf{3.8 \times 10^{17}}$	0.00192	0.28047	0.12824 ± 0.006

As above, we measured the time-resolved anisotropy decay of these mats at different doping densities (Figure 3c). The results show a rapid decay in the measured anisotropy for all the doped mats. In contrast to the measurements taken with solvated proteins, where the slow rotation of the

protein resulted in a slow time component following the Homo-FRET process (τ_2 in Table 1), in the solid matrix, we do not expect to see any depolarization due to slow rotation events. Indeed, the results show a rapid decay, followed by a constant anisotropy. This finding also validates our assertion that Flu molecules are strongly bound to the protein matrix and not leached to water (the BSA mat has a water content of up to 150 wt.%) within the protein matrix.[14, 15] Furthermore, the anisotropy measured for the wet matrix was highly similar to that of a dry matrix (Figure S3); thus, the results demonstrated that the presence of Homo-FRET between fluorophores situated within the proteins in the matrix was what we observed.

We can treat our results of the time-resolved anisotropy curve for samples experiencing heavily restricted rotation in a solid platform as a transition from an initial anisotropy value r_0 to a non-zero asymptote, denoted as r_∞:

$$r(t) = r_\infty + A_{FRET} \cdot e^{-\left(\frac{t}{\tau_3}\right)} \quad (7)$$

The fitting parameters are summarized in Table 2. As the dopant density increases, the decay amplitude (A_{FRET}) increases, indicating the increased involvement of Flu molecules that exchange energy. A similar finding was found in a study where the concentration of labeled proteins within amyloid fibrils was increased.[34] At the highest concentration tested, referred to as 'full doping', we achieved complete depolarization, as can be observed by the nil anisotropy value. In other words, when the surface was excited with a beam of a specific polarization, the emitted light polarization was uniformly received from all directions. This phenomenon occurs because elevating the concentration of fluorophores results in a broader distribution of fluorophores with diverse spatial orientations and proximity, thus giving rise to efficient energy transfer.

Two intriguing findings from the anisotropy measurements of the doped surfaces are 1) a similar anisotropy starting value (which we refer to above as r_0) for all doping densities and 2) a similar energy transfer decay (τ_3) for all doping densities. These findings imply that a similar Homo-FRET

mechanism is shared among all our solid matrix samples. However, these findings contrast with the measurements performed with the solvated protein, whereas we observed a decrease in r_0 and a decrease in the decay value as a function of the concentration of the Flu molecule within a single protein. Nevertheless, it is important to note that the similar decay observed for the Homo-FRET process within the protein matrix (τ_3) for all doping densities is similar to the value obtained for the Homo-FRET process within the solvated proteins but only at ratios above BSA 1:4 Flu (τ_1 in Table 1). Moreover, above this BSA:Flu ratio, we also did not observe a change in r_0 as a function of the ratio. This similarity indicates that the mechanism of action of Homo-FRET within the protein matrix, regardless of the doping density, is likely similar to the mechanism involving solvated proteins at large copy numbers of the fluorophores. Hence, we suggest here that regardless of the doping density, the delocalization of energy occurs over several fluorophores, and increasing the density further does not improve this process. However, increasing the doping density allows more fluorophores to participate in the hopping process, eventually resulting in the full depolarization observed in the fully doped matrix.

In summary, we followed the Homo-FRET process between Flu molecules situated within the BSA protein either in its freely solvated form or in a solid protein matrix using fluorescence anisotropy measurements. For the solvated protein, we showed that the number of Flu molecules within the protein strongly influenced all the parameters of the Homo-FRET process, including the rate of energy transfer and its amplitude. We observed two unexpected findings: 1) a reduction in the limiting anisotropy and 2) a greater-than-ideal contribution of Homo-FRET to the measured fluorescence anisotropy. Our observations might suggest that coherent energy transfer processes are involved in the observed Homo-FRET; thus, a mixed coherent-incoherent (hopping) mechanism is suggested. Unlike the measurements with solvated protein, the Homo-FRET anisotropy measurements within the solid protein matrix showed similar anisotropy decay and limiting anisotropy for all the different concentrations of Flu within the matrix, and only the long timescale

anisotropy was slowly reduced to approximately zero at high doping densities. The similar values of both the anisotropy decay and the limiting anisotropy to the values obtained with the solid protein matrix suggest a similar mechanism regardless of the doping density. The reduction in the long timescale anisotropy might imply that the delocalization spreads over longer distances within the solid matrix at high doping densities.

Supporting Information

Experimental Section and Supporting Figures (Figures S1-S3) can be found online.

Acknowledgments

Y.A. thanks the Russel Berrie Nanotechnology Institute RBNI Scholarship for financial support. N.A. thanks the Ministry of Science and Technology (number 3-16312). We thank the Grand Technion Energy Program (GTEP) and the Russel Berrie Nanotechnology Institute (RBNI) for their support in equipment use.

References

1. Szabó, Á.; Szöllősi, J.; Nagy, P., Principles of Resonance Energy Transfer. *Current Protocols* **2022,** *2* (12), e625.
2. Gautier, I.; Tramier, M.; Durieux, C.; Coppey, J.; Pansu, R. B.; Nicolas, J. C.; Kemnitz, K.; Coppey-Moisan, M., Homo-FRET Microscopy in Living Cells to Measure Monomer-Dimer Transition of GFP-Tagged Proteins. *Biophysical Journal* **2001,** *80* (6), 3000-3008.
3. Tao, M.-J.; Zhang, N.-N.; Wen, P.-Y.; Deng, F.-G.; Ai, Q.; Long, G.-L., Coherent and incoherent theories for photosynthetic energy transfer. *Science Bulletin* **2020,** *65* (4), 318-328.
4. Nelson, N.; Junge, W., Structure and Energy Transfer in Photosystems of Oxygenic Photosynthesis. *Annual Review of Biochemistry* **2015,** *84* (1), 659-683.

5. Colbow, K., Energy transfer in photosynthesis. *Biochim. Biophys. Acta* **1973,** *314* (3), 320-327.

6. Chenu, A.; Scholes, G. D., Coherence in Energy Transfer and Photosynthesis. *Annual Review of Physical Chemistry* **2015,** *66* (1), 69-96.

7. Engel, G. S.; Calhoun, T. R.; Read, E. L.; Ahn, T.-K.; Mančal, T.; Cheng, Y.-C.; Blankenship, R. E.; Fleming, G. R., Evidence for wavelike energy transfer through quantum coherence in photosynthetic systems. *Nature* **2007,** *446* (7137), 782-786.

8. Lee, H.; Cheng, Y.-C.; Fleming, G. R., Coherence Dynamics in Photosynthesis: Protein Protection of Excitonic Coherence. *Science* **2007,** *316* (5830), 1462-1465.

9. Mohseni, M.; Rebentrost, P.; Lloyd, S.; Aspuru-Guzik, A., Environment-assisted quantum walks in photosynthetic energy transfer. *Chem. Phys.* **2008,** *129* (17).

10. Ishizaki, A.; Calhoun, T. R.; Schlau-Cohen, G. S.; Fleming, G. R., Quantum coherence and its interplay with protein environments in photosynthetic electronic energy transfer. *Phys. Chem. Chem. Phys.* **2010,** *12* (27), 7319-7337.

11. Schlau-Cohen, G. S.; Calhoun, T. R.; Ginsberg, N. S.; Read, E. L.; Ballottari, M.; Bassi, R.; van Grondelle, R.; Fleming, G. R., Pathways of Energy Flow in LHCII from Two-Dimensional Electronic Spectroscopy. *The Journal of Physical Chemistry B* **2009,** *113* (46), 15352-15363.

12. Chenu, A.; Christensson, N.; Kauffmann, H. F.; Mančal, T., Enhancement of Vibronic and Ground-State Vibrational Coherences in 2D Spectra of Photosynthetic Complexes. *Sci. Rep.* **2013,** *3* (1), 2029.

13. Dror, Y.; Ziv, T.; Makarov, V.; Wolf, H.; Admon, A.; Zussman, E., Nanofibers Made of Globular Proteins. *Biomacromolecules* **2008,** *9* (10), 2749-2754.

14. Agam, Y.; Nandi, R.; Bulava, T.; Amdursky, N., The role of the protein–water interface in dictating proton conduction across protein-based biopolymers. *Materials Advances* **2021,** *2* (5), 1739-1746.

15. Amdursky, N.; Wang, X.; Meredith, P.; Bradley, D. D. C.; Stevens, M. M., Long-Range Proton Conduction across Free-Standing Serum Albumin Mats. *Adv. Mater.* **2016,** *28* (14), 2692-2698.

16. Silori, Y.; De, A. K., Controlling balance between Homo-FRET and hetero-FRET within hetero-chromophoric systems by tuning nature of solvent. *J. Mol. Liq.* **2020,** *298*, 112093.

17. Andersson, L.-O.; Rehnström, A.; Eaker, D. L., Studies on "Nonspecific" Binding. *European Journal of Biochemistry* **1971,** *20* (3), 371-380.

18. Tramier, M.; Coppey-Moisan, M., Fluorescence Anisotropy Imaging Microscopy for Homo-FRET in Living Cells. In *Methods in Cell Biology*, Academic Press: 2008; Vol. 85, pp 395-414.

19. Ghosh, S.; Saha, S.; Goswami, D.; Bilgrami, S.; Mayor, S., Chapter sixteen - Dynamic Imaging of Homo-FRET in Live Cells by Fluorescence Anisotropy Microscopy. In *Methods Enzymol.*, Conn, P. M., Ed. Academic Press: 2012; Vol. 505, pp 291-327.

20. Ojha, N.; Rainey, K. H.; Patterson, G. H., Imaging of fluorescence anisotropy during photoswitching provides a simple readout for protein self-association. *Nature Communications* **2020,** *11* (1), 21.

21. Esposito, A.; Bader, A. N.; Schlachter, S. C.; van den Heuvel, D. J.; Schierle, G. S. K.; Venkitaraman, A. R.; Kaminski, C. F.; Gerritsen, H. C., Design and application of a confocal microscope for spectrally resolved anisotropy imaging. *Optics Express* **2011,** *19* (3), 2546-2555.

22. Smith, T. A.; Ghiggino, K. P., A review of the analysis of complex time-resolved fluorescence anisotropy data. *Methods and Applications in Fluorescence* **2015,** *3* (2), 022001.

23. Agarwal, A.; Das, D.; Banerjee, T.; Mukhopadhyay, S., Energy migration captures membrane-induced oligomerization of the prion protein. *Biochim. Biophys. Acta* **2020,** *1868* (2), 140324.

24. Lakowicz, J. R., *Principles of fluorescence spectroscopy*. Springer: 2006.

25. Magde, D.; Wong, R.; Seybold, P. G., Fluorescence Quantum Yields and Their Relation to Lifetimes of Rhodamine 6G and Fluorescein in Nine Solvents: Improved Absolute Standards for Quantum Yields¶. *Photochem. Photobiol.* **2002,** *75* (4), 327-334.

26. Paul, B. K.; Ghosh, N.; Mukherjee, S., Interplay of Multiple Interaction Forces: Binding of Norfloxacin to Human Serum Albumin. *The Journal of Physical Chemistry B* **2015,** *119* (41), 13093-13102.

27. Paul, B. K.; Guchhait, N., Modulated Photophysics of an ESIPT Probe 1-Hydroxy-2-naphthaldehyde within Motionally Restricted Environments of Liposome Membranes Having Varying Surface Charges. *The Journal of Physical Chemistry B* **2010,** *114* (39), 12528-12540.

28. Chan, F. T. S.; Kaminski, C. F.; Kaminski Schierle, G. S., HomoFRET Fluorescence Anisotropy Imaging as a Tool to Study Molecular Self-Assembly in Live Cells. *ChemPhysChem* **2011,** *12* (3), 500-509.

29. Bader, A. N.; Hoetzl, S.; Hofman, E. G.; Voortman, J.; van Bergen en Henegouwen, P. M.; van Meer, G.; Gerritsen, H. C., Homo-FRET imaging as a tool to quantify protein and lipid clustering. *Chemphyschem* **2011,** *12* (3), 475-83.

30. Maus, M.; Mitra, S.; Lor, M.; Hofkens, J.; Weil, T.; Herrmann, A.; Müllen, K.; De Schryver, F. C., Intramolecular Energy Hopping in Polyphenylene Dendrimers with an Increasing Number of Peryleneimide Chromophores. *The Journal of Physical Chemistry A* **2001,** *105* (16), 3961-3966.

31. Varnavski, O. P.; Ostrowski, J. C.; Sukhomlinova, L.; Twieg, R. J.; Bazan, G. C.; Goodson, T., Coherent Effects in Energy Transport in Model Dendritic Structures Investigated by Ultrafast Fluorescence Anisotropy Spectroscopy. *J. Am. Chem. Soc.* **2002,** *124* (8), 1736-1743.

32. Agam, Y.; Nandi, R.; Kaushansky, A.; Peskin, U.; Amdursky, N., The porphyrin ring rather than the metal ion dictates long-range electron transport across proteins suggesting coherence-assisted mechanism. *Proc. Natl. Acad. Sci. U.S.A.* **2020,** *117* (51), 32260-32266.

33. Amdursky, N.; Wang, X.; Meredith, P.; Riley, D. J.; Payne, D. J.; Bradley, D. D. C.; Stevens, M. M., Electron Hopping Across Hemin-Doped Serum Albumin Mats on Centimeter-Length Scales. *Adv. Mater.* **2017,** *29* (27), 1700810.

34. Majumdar, A.; Mukhopadhyay, S., Excitation energy migration to study protein oligomerization and amyloid formation. *Biophysical Chemistry* **2022,** *281*, 106719.